Applied Catalysis B: Environmental 189 (2016) 252–265

Contents lists available at ScienceDirect

Applied Catalysis B: Environmental

journal homepage: www.elsevier.com/locate/apcatb

Supported $H_3PW_{12}O_{40}$ for 2-propanol (photo-assisted) catalytic dehydration in gas-solid regime: The role of the support and of the pseudo-liquid phase in the (photo)activity

Elisa I. García-López[a], Giuseppe Marcì[a,*], Francesca Rita Pomilla[a], Aleksandra Kirpsza[b], Anna Micek-Ilnicka[b], Leonardo Palmisano[a]

[a] "Schiavello-Grillone" Photocatalysis Group. Dipartimento di Energia, Ingegneria dell'informazione e modelli Matematici (DEIM), Università di Palermo, Viale delle Scienze, 90128 Palermo, Italy
[b] Jerzy Haber Institute of Catalysis and Surface Chemistry Polish Academy of Sciences, ul. Niezapominajek 8, 30-239 Kraków, Poland

ARTICLE INFO

Article history:
Received 17 December 2015
Received in revised form 22 February 2016
Accepted 27 February 2016
Available online 3 March 2016

Keywords:
Heteropolyacid
2-Propanol dehydration
Photocatalysis
Pseudo-liquid phase
Keggin

ABSTRACT

Catalytic and photocatalytic 2-propanol dehydration was carried out by using a supported Keggin heteropolyacid $H_3PW_{12}O_{40}$ (PW_{12}). Binary materials were prepared by impregnation and/or solvothermal treatment by using commercial supports: SiO_2 (Mallinckrodt), TiO_2 (Evonik P25) and multiwall carbon nanotubes (Sunnano) or home solvothermically prepared SiO_2 and TiO_2. All the materials have been characterized by X-ray diffraction (XRD), scanning electron microscopy observations (SEM) coupled with EDX microanalysis, specific surface area measurements, diffuse reflectance spectroscopy (DRS), FTIR and Raman spectroscopy. (Photo)catalytic 2-propanol dehydration was studied in gas-solid regime by using a continuous (photo)reactor working at atmospheric pressure and 80 °C. FTIR spectra of the gas-phase over the PW_{12}-support composites, where 2-propanol had been previously adsorbed, were recorded. Propene and diisopropyl ether were the main reaction products. For the continuous photo-assisted runs the reactor was also illuminated with UV light. The apparent activation energy of 2-propanol catalytic and photocatalytic dehydration was determined in the range 60–120 °C.

The irradiance increased significantly the dehydration reaction rate. Important differences were observed between the different supported materials. The Keggin heteropolyacid species played a key role both for the catalytic and the photo-assisted catalytic reactions; in fact, the acidity of the cluster accounts for the catalytic role, whereas both the acidity of the cluster and the oxidant ability of PW_{12} were responsible for the increase of the reaction rate of the photo-assisted catalytic reaction. Moreover, the photo-generated electrons on the solid semiconductor conduction band can account for a further increase of the reaction rate, when the heteropolyacid was supported on TiO_2. Formation of a pseudo-liquid phase played an important role to determine the (photo)activity.

1. Introduction

Polyoxometalates (POMs) are a wide class of discrete nanosized transition metal oxygen clusters. Metal oxides can be subdivided into classical solid oxides and molecular metal oxide clusters: POMs that offer a fascinating range of structures and properties [1]. POMs can be divided in three classes: heteropolyanions, isopolyanions and Mo-blue and Mo-brown reduced heteropolyanions centers [2]. The most explored POM materials are the heteropolyacids and it is convenient to classify them starting from the symmetrical 'parent' polyanion, for instance the Keggin or Wells-Dawsons structures among others. The Keggin anion $\{XM_{12}O_{40}\}$ contains a heteroatom X in the XO_4^- center as PO_4^{3-} or SiO_4^{3-} and the so-called addenda atoms, commonly W or Mo. For instance, the structure of the $PW_{12}O_{40}^{3-}$ anion consists of a PO_4 tetrahedron surrounded by four W_3O_9 groups formed by edge sharing octhaedra. This cluster has a diameter of ca. 1.0 nm. The heteropolyacids with the Keggin structure are strongly acidic and are remarkably stable particularly when deposited onto large oxide surfaces. They are widely used in homo- and heterogenous catalysis and also as photocatalysts in homogeneous systems, due to their solubility in polar solvents [3].

Heteropolyacids (HPA) can be used as photocatalysts because they absorb light by the ground electronic state producing a charge transfer-excited state (HPA*). The HPA* species act as better oxidant

* Corresponding author.
E-mail address: giuseppe.marci@unipa.it (G. Marcì).

http://dx.doi.org/10.1016/j.apcatb.2016.02.063
0926-3373/

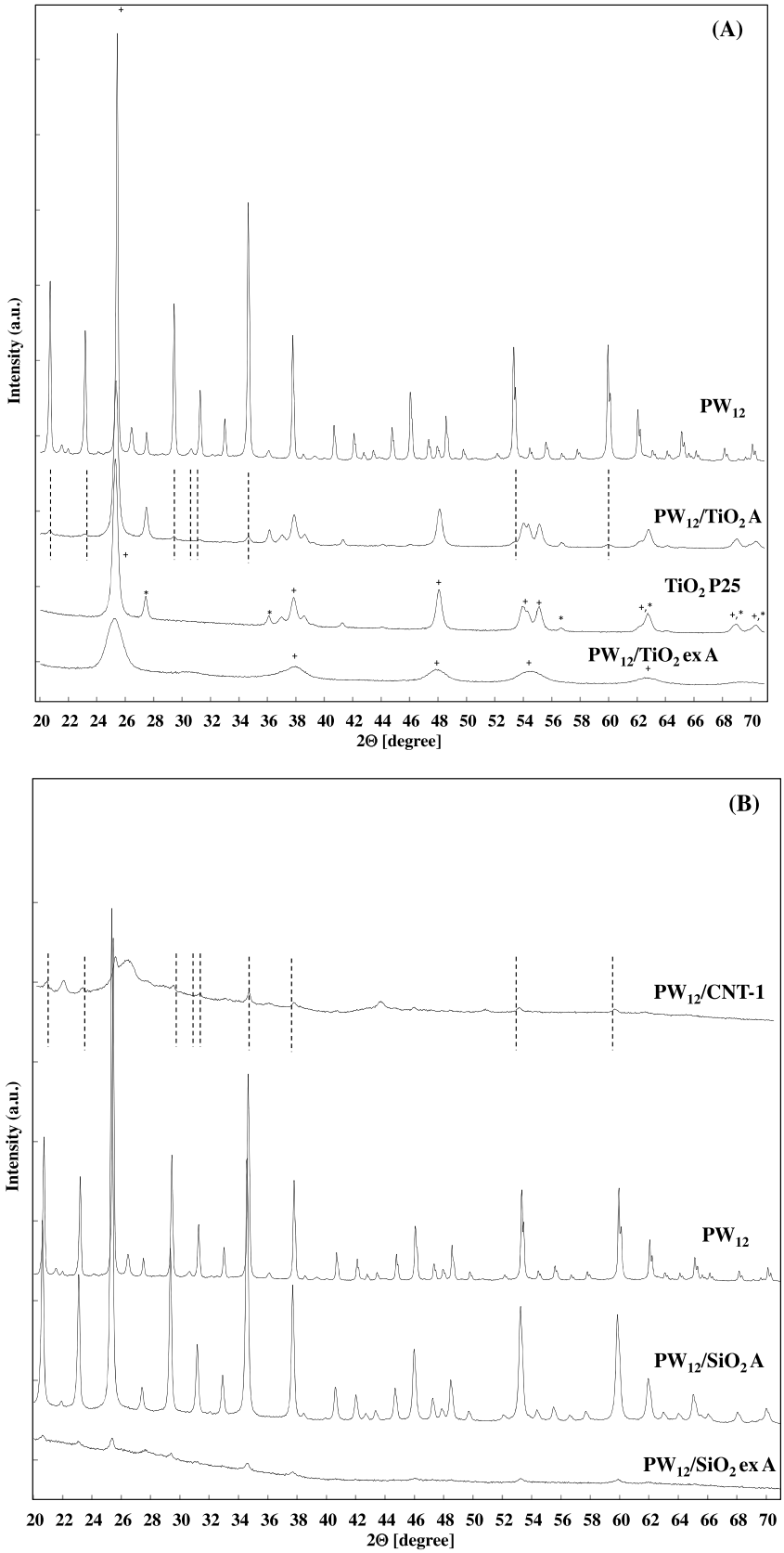

Fig. 1. XRD patterns of the photocatalysts: (A) bare PW_{12} along with bare TiO_2 and their binary materials. (⋆ Rutile; + Anatase) and (B) bare PW_{12} along with binary materials composed of SiO_2 and PW_{12} and a representative composite composed of PW_{12} and CNT.

and reductant than the corresponding ground states [4]. Indeed, HPA* can easily become HPA^{-}, the so-called "heteropolyblue" by means of one (or more) electron transfer from another species [5]. Heteropolyblues (HPA^{n-}) are relatively stable and are readily re-oxidised. The enhanced degradation of organic compounds in the UV/TiO_2 process in the presence of supported Keggin-type HPAs has been reported [6]. In a previous paper, the catalytic and catalytic photo-assisted activity of $H_3PW_{12}O_{40}$ supported on TiO_2, ZrO_2 or WO_3 was studied and a beneficial role of the photoactive support on the reaction rate was observed [7]. The dispersion of HPAs on solid supports with high surface area is useful to improve the accessibility to their acid sites, and consequently to increase their catalytic activity. The significant increase of reactivity in the photocatalytic process has been justified by considering the ability of the semiconductor to transfer electrons from the conduction band to the activated HPA^{*} species. In fact, TiO_2 can directly transfer photogenerated electrons from its conduction band to the interfacial HPA with empty d orbitals. By using coupled HPA/TiO_2 materials in heterogeneous photocatalysis, the rate of conduction band (CB) electron transfer is enhanced, and consequently the charge-pair recombination is delayed [8].

In this paper the catalytic and catalytic photo-assisted 2-propanol reaction in gas-solid regime has been carried out by using as the (photo) catalysts samples containing $H_3PW_{12}O_{40}$ deposited on SiO_2, TiO_2 or multiwall carbon nanotubes (CNT). The deposition has been done on commercial supports by impregnation under ambient or hydrothermal experimental conditions. Moreover, alternative binary materials have been prepared by a solvothermal method from Ti or Si alkoxydes in aqueous solutions containing PW_{12}. The amount of the heteropolyacid present in the binary material along with the physico-chemical features of the support strongly influenced the (photo) catalytic activity of these solids.

The dehydration of 2-propanol to form propene is considered a useful reaction to characterize the acidity of a catalyst [9]. In a gas-solid regime propene and/or propanone are formed at ambient pressure and moderate temperature (in the range 140–325 °C) [10–12]. The selectivity to these products mainly depends on the acidity-basicity of the solid catalyst. Some bulk and surface properties of the catalysts have been studied and the effect of light has been investigated by taking into account that the (photo) reactivity can depend on the features of the support and the formation of a pseudo-liquid phase, both related to the presence of HPA.

2. Experimental

2.1. Preparation of the binary heteropolyacid/support samples

Three sets of catalysts have been prepared by using the commercial heteropolyacid (HPA), tungstophosphoric acid $H_3PW_{12}O_{40}$ (Aldrich reagent grade 99.7%), named PW_{12} in the following, and three kind of supports i.e.: SiO_2, TiO_2 and multiwall carbon nanotubes, in the following named CNTs.

2.1.1. Binary PW_{12}/SiO_2 samples

It is worth to mention that the theoretical coverage of the support has been calculated by taking into account that the diameter of each PW_{12} anionic cluster is equal to ca. 10 Å and, consequently, by considering a roundish shape of the heteropolyanion, the surface area covered by each cluster was ca. 78.5 $Å^2$ [13].

An aqueous solution of PW_{12} has been used to impregnate a commercial SiO_2 (100 mesh, A.R. Mallinckrodt). In order to obtain ca. a theoretical monolayer of PW_{12} onto the SiO_2 surface, it was chosen a molar ratio Si: PW_{12} equal to $0.013{:}6.9 \times 10^{-4}$. The impregnation has been carried out under hydrothermal conditions at 200 °C for 48 h in an autoclave provided with a Teflon beaker. The resulting solid was filtered and dried at 40° overnight and it was labeled PW_{12}/SiO_2 A, where A indicates the hydrothermal treatment.

A bare SiO_2 powder has been prepared by a hydrothermal treatment (48 h at 200 °C) of an aqueous solution of tetraethylortosilicate (TEOS) used as the SiO_2 precursor. It was labeled as SiO_2 hp (home prepared).

An alternative binary material PW_{12}/SiO_2 has been prepared by adding TEOS to an aqueous suspension containing an amount of PW_{12} corresponding to a molar ratio Si: PW_{12} equal to $0.103{:}6.9 \times 10^{-4}$. The resulting sample has been labeled as PW_{12}/SiO_2 ex A.

2.1.2. Binary PW_{12}/TiO_2 samples

A second set of samples was prepared by using TiO_2 as the HPA support under hydrothermal conditions (48 h, 200 °C). An aqueous solution containing PW_{12} was used to impregnate the surface of the commercial TiO_2 Evonik P25. The molar ratio Ti: PW_{12} was $0.103{:}6.9 \times 10^{-4}$. The obtained solid was filtered and dried overnight and eventually labeled PW_{12}/TiO_2 A. Moreover, a home prepared TiO_2 (TiO_2 hp) was obtained by using titanium isopropoxide (Aldrich 97%), $Ti(OPr)_4$, that was hydrolyzed in water and the resulting suspension was hydrothermally treated for 48 h at 200 °C, filtered and dried. A solution of titanium isopropoxide was also hydrolyzed in an aqueous solution of PW_{12} (the molar ratio Ti: PW_{12} was the same of the previous sample i.e. $0.103{:}6.9 \times 10^{-4}$). The resulting suspension was treated in autoclave for 48 h at 200 °C, filtered, dried and the obtained solid was labeled as PW_{12}/TiO_2 ex A.

2.1.3. Binary PW_{12}/Carbon nanotubes (CNT) samples

Two samples have been prepared by depositing HPA on carbon nanotubes (CNT). PW_{12}/CNT samples were prepared by using multiwall carbon nanotubes CNT (Sun Nanotech Co) and PW_{12}. Before synthesis both components, carbon nanotubes and heteropolyacid, were dehydrated by heating. The former was heated at 353 K for 1 h and the latter at 483 K for 2 h. Two binary materials were prepared by using an amount of PW_{12} which corresponded to the theoretical coverage of the CNT support with approximately 1.0 or 0.5 layers of the clusters. The samples were labeled as PW_{12}/CNT-1 and PW_{12}/CNT-0.5 where the values 1 and 0.5 denote the PW_{12} coverage. To prepare these materials an appropriate amount of anhydrous $H_3PW_{12}O_{40}$ was dissolved in absolute ethanol (10 to 30 mL) and stirred for 3 h with the CNT powder. The suspension was evaporated at room temperature and dried at 60 °C for 2 h.

Table 1 reports the prepared powders with their acronyms, their specific surface areas, and the relative amount of the components.

2.2. Characterization of the binary heteropolyacid/support samples

Bulk and surface characterizations were carried out in order to define some physicochemical properties of the powders. Raman measurements were performed on pure powdered samples. Spectra were recorded by a Reinshaw in-via Raman equipped with an integrated microscope and with a charged-coupled device (CCD) camera. A He/Ne laser operating at 632.8 nm was used as the exciting source. The crystalline structure of the samples was determined at room temperature by powder X-ray diffraction analysis (PXRD) carried out by using a Panalytical Empyrean, equipped with CuKa radiation and PixCel1D (tm) detector. Specific surface area was determined in accordance with the standard Brunauer-Emmet-Teller (BET) method from the nitrogen adsorption-desorption isotherm using a Quantasorb Jr. The total content of water in the catalysts was roughly measured by Moisture Analyzer MAC50

Table 1
Specific surface areas (SSA), amount of PW_{12} and support in each sample and theoretical PW_{12} coverage on the support for the binary materials.

Sample	SSA [$m^2\ g^{-1}$]	Mass PW_{12} [%]	Mass support [%]	Theoreticalcoverage
SiO_2	517	–	100	–
SiO_2 hp	116	–	100	–
PW_{12}	15	–	–	–
PW_{12}/SiO_2 A	32	74	26	0.8
PW_{12}/SiO_2 ex A	219	27	73	0.5
TiO_2 Evonik P25	50	–	100	–
TiO_2 hp	161	–	100	–
PW_{12}/TiO_2 A	43	22	78	0.8
PW_{12}/TiO_2 ex A	161	22	78	0.2
CNT	138	–	100	–
PW_{12}/CNT-1	85	39	61	1
PW_{12}/CNT-0.5	91	14	86	0.4

Table 2
Apparent activation Energy (E_a) and logarithm of the pre-exponential factor (ln A) for catalytic and photocatalytic 2-propanol dehydration.

Catalyst	E_a [kJ/mol]		ln A	
	Catalytic	Photocatalytic	Catalytic	Photocatalytic
PW_{12}	186	157	57.6	51.5
PW_{12}/TiO_2 A	161	125	52.5	42.9
PW_{12}/SiO_2 A	145	128	45.8	40.8
PW_{12}/CNT-0.5	165	140	53.8	47.6

Radwag. FTIR spectroscopy allowed to control the retention of Keggin anions throughout the catalysts synthesis and the continuous observation of reaction substrate, intermediate species and products. The preservation of the Keggin structure during the runs and the continuous observation of reaction substrates, intermediates and products was carried out in situ by FTIR spectroscopy. The FTIR spectra was recorded using *Excalibur 300 Series Digilab* spectrometer, equipped with DTGS detector at 4 cm^{-1} spectral resolution in the MID-IR range (4000–400 cm^{-1}). The preparation of the samples for IR measurements consisted of several steps: a few drops of an aqueous suspension of sample were deposited onto silicon wafers, then the excess of solvent was evaporated under ambient conditions. The wafers were placed in a home-made glass holder (handle) in the vertical position which ensured the perpendicular position of the sample with respect to the IR beam. This holder was provided with a magnet which allowed the easy moving of the sample from the oven (outside the IR beam) into the IR cell. This cell was closed with thallium bromoiodide (KRS-5) windows.

2.3. Catalytic experiments

2.3.1. *Infra-red monitoring of 2-propanol dehydration:* system I

Catalytic experiments were carried out in an infrared cell, used as a batch catalytic reactor, connected to the sorption setup which allowed to dose the vapour of 2-propanol at known pressures and controlled temperature. All spectra were measured at ambient temperature, because the oven was located in other part of the cell. The samples (ca. 0.01 g) were evacuated for 5 min at r.t. prior to 2-propanol sorption, and the pressure of adsorbate was 1.3 kPa. Then the temperature was stepwise raised from r.t. to 140 °C and the spectra were recorded after reaction with 2-propanol at 40, 60, 80, 100, 120 and 140 °C. *System I* allowed to continuously monitor both the catalyst surface and the gas phase.

2.3.2. *Catalytic and catalytic photo-assisted experiments:* system II

An alternative set-up consisting of a cylindrical continuous Pyrex photoreactor horizontally positioned (diameter: 10 mm, length: 100 mm) was used and it operated in gas-solid regime. The reactivity runs were carried out with 0.5 g of solid powder by placing it as a thin layer inside the photoreactor (the fixed bed height was ca. 0.3 mm). A porous glass septum allowed to homogeneously distribute the gaseous inlet mixture consisting of a nitrogen flow containing 2-propanol with molar concentration ranging between ca. 0.1 and 3.0 mM. A mass flow controller allowed to feed N_2, whereas 2-propanol was mixed with the N_2 stream by means of a home assembled infusion pump. The flow rate of the gaseous stream for the catalytic and catalytic photo-assisted runs was in the range 20–100 ml min^{-1}. All the runs were carried out at atmospheric pressure. The reactor and the pipes of the set-up to and from the reactor were heated by an electric resistance and K-type thermocouples allowed to monitor the temperature in the whole system. The temperature inside the (photo)-reactor was modified in the range 60–120 °C, whereas for most of the runs it was maintained constant at 80 °C both for catalytic and catalytic photo-assisted experiments. For the catalytic photo-assisted runs the reactor was illuminated from the top with one or two UV LED IRIS 40 lamps with an irradiation peak centred at 365 nm. The irradiance reaching the photoreactor was measured in the range 300–400 nm with a UVX Digital radiometer, and it resulted 0.28 W and 0.50 W when one or two LEDs, respectively, were switched on. The temperature of the photoreactor was maintained constant during the irradiation. The runs lasted ca. 8 h and samples of the reacting fluid were analyzed by a Shimadzu 17A gas chromatograph equipped with an Alltech AT-1 (30 m, 0.53 mm, 2.65 μm) column (oven temperature 40 °C) and a FID.

3. Results and discussion

3.1. Bulk and textural photocatalysts characterization

XRD diffractograms of all of the samples are reported in Fig. 1. The diffractograms of bare PW_{12}, commercial and home prepared TiO_2, PW_{12}/TiO_2 A and PW_{12}/TiO_2 ex A are reported in Fig. 1(A). PW_{12} presents a crystalline structure characterized by several diffraction peaks. In the diffractogram of the commercial TiO_2 P25, anatase and rutile polymorphs can be identified, whereas for the bare home prepared TiO_2 only the presence of anatase phase was noticed.

In the composite materials, peaks attributable to the heteropolyacid and to TiO_2 are present and they are less intense in the PW_{12}/TiO_2 ex A than in the PW_{12}/TiO_2 A. This finding can account

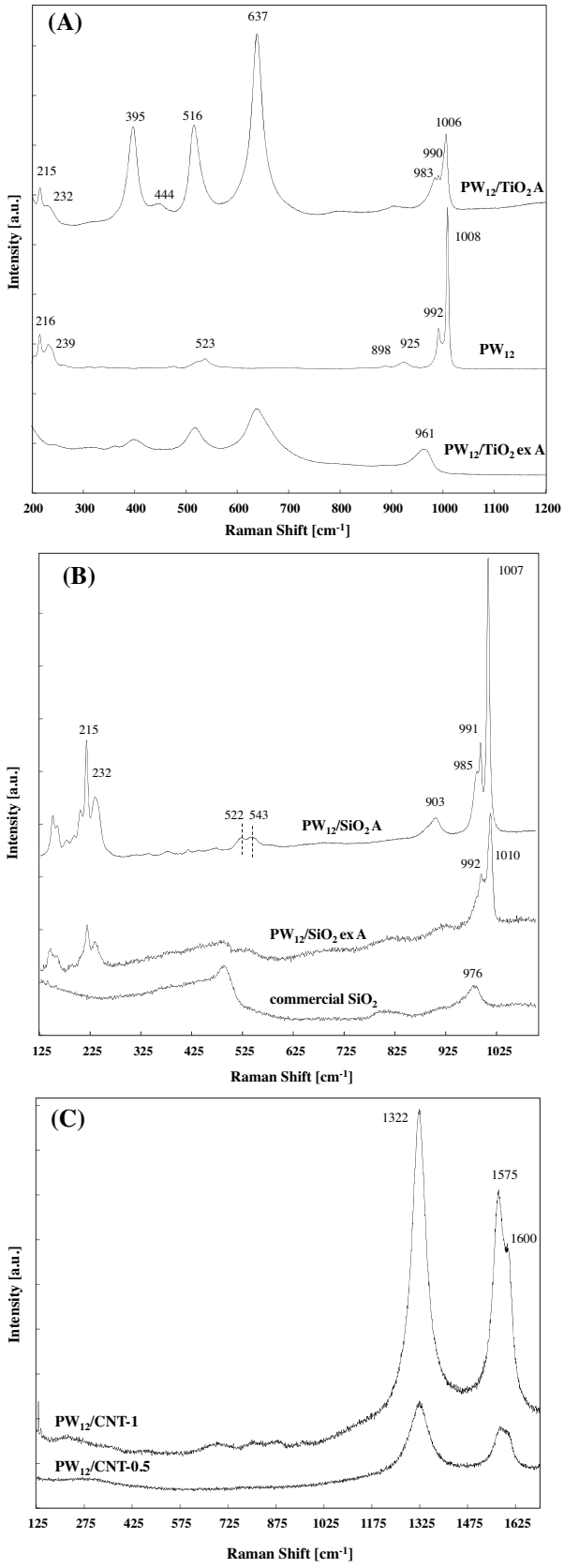

Fig. 2. Raman spectra of the samples: (A) bare PW_{12} and PW_{12}/TiO_2 binary materials; (B) commercial SiO_2 and PW_{12}/SiO_2 binary materials and (C) PW_{12}/CNT composites.

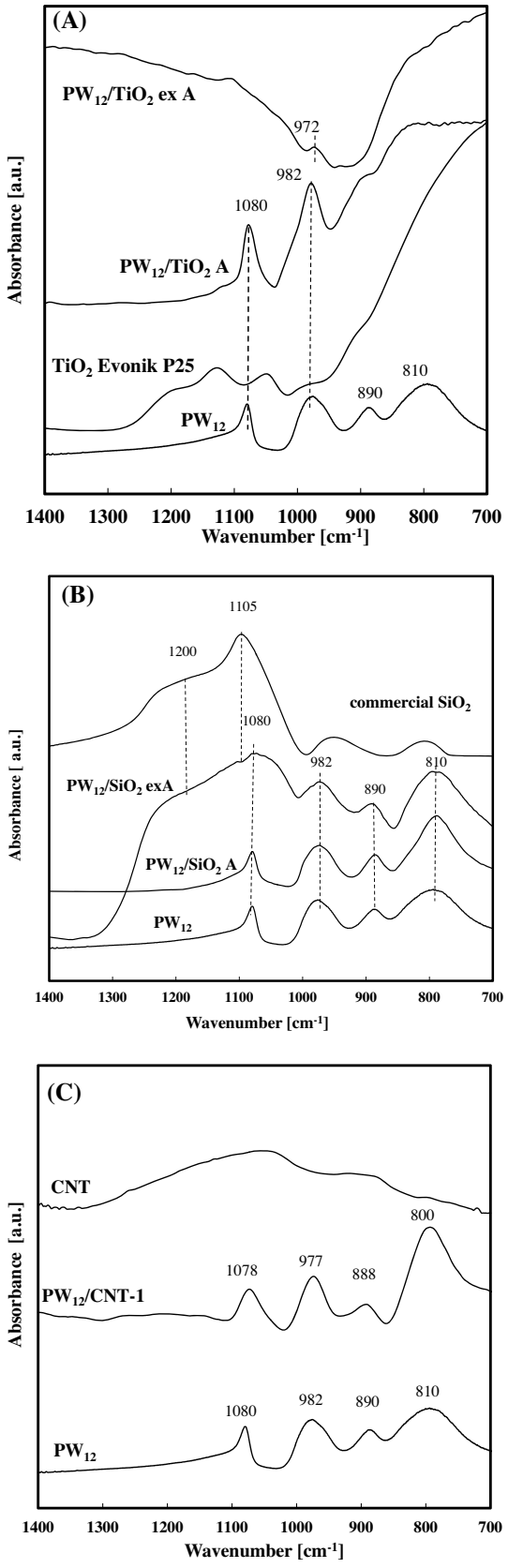

Fig. 3. FTIR spectra of the following samples: (A) commercial TiO_2 Evonik P25, bare PW_{12} and PW_{12}/TiO_2 binary materials; (B) commercial SiO_2 and its composites with PW_{12} and (C) bare CNT and PW_{12}/CNT-1. All the spectra were recorded after *in-situ* evacuation of the samples at room temperature for 5 min. (Set-up *system I*).

for the best dispersion of the PW_{12} in the material prepared solvothermically. Indeed, the more defined peaks can be due to the heterogeneity of the dispersion of the HPA in the PW_{12}/TiO_2 A sample, as confirmed by SEM (see Supplementary material). Fig. 1(B) shows the diffractogram of PW_{12} along with those of the samples based on SiO_2 and CNT. Both commercial and SiO_2 hp pristine samples were completely amorphous, so binary materials PW_{12}/SiO_2 A and PW_{12}/SiO_2 ex A showed diffraction peaks attributable only to the presence of the PW_{12} cluster. For the first sample the diffractogram suggests a good crystallinity of the Keggin cluster and the presence of bigger crystallites. The diffraction pattern of PW_{12}/CNT-1 showed only peaks ascribable to the PW_{12} presence.

As reported in Table 1, specific surface areas (SSA) of PW_{12} impregnated samples decreased with respect to the bare commercial supports. This finding can be attributed to the fact that some pores of the supports are blocked, due to the presence of the heteropolyacid clusters and this phenomenon was particularly evident in the case of PW_{12}/SiO_2 A for which the SSA decreases from 517 to 32 $m^2\,g^{-1}$. On the contrary, it is remarkable that SSA of the materials prepared by mixing the Si or Ti alkoxyde with $PW_{12,}$ i.e. the PW_{12}/SiO_2 ex A or PW_{12}/TiO_2 ex A, does not change significantly compared to the bare hydrothermally prepared bare oxides, indicating that the heteropolyacid has been incorporated into the porous structure of the binary system without reducing the porosity of the bare oxide. It is worth to note that the SSA of the PW_{12}/SiO_2 ex A sample results higher than that of SiO_2 hp probably because during the hydrolysis of TEOS (the SiO_2 precursor) the formed ethanol, reacting with PW_{12}, gave rise to a slow evolution of ethene that favoured the porosity of the sample. The evolution of gas (propene) was instead observed during the preparation of the PW_{12}/TiO_2 ex A sample, but it was not able to increase the SSA with respect to the bare TiO_2 hp. The surface areas of PW_{12}/CNT-0.5 and PW_{12}/CNT-1 samples were very similar each other but lower than that of the bare CNT. Consequently, it is plausible that PW_{12} not only partially covered the nanotubes surface reducing the SSA but also filled or clogged their pores. As a general trend, the surface areas of the binary materials are smaller than those of the bare supports.

Fig. 2(A–C) shows the Raman spectra of bare and supported PW_{12} samples. Spectra of bare TiO_2 samples (not reported for the sake of brevity) show bands at 395, 516 and 637 cm^{-1} characteristic of anatase crystalline phase [14]. A peak attributed to the rutile phase is also present and located at 444 cm^{-1} [14]. Intense peaks at 142 and 144 cm^{-1}, assigned to rutile and anatase, respectively, are out of the range of the spectra reported in Fig. 2. In the spectrum of PW_{12} sample four characteristic bands at 1008 cm^{-1} (assigned to the ν_s W—O_d vibration), at 992 cm^{-1} (assigned to the ν_{as} W—O_d vibration) [15,16], and at 925 cm^{-1} and 898 cm^{-1} (attributed to W—O_b—W and W—O_c—W vibrations), are present [16]. The weaker bands reported in Fig. 2(A) for the bare PW_{12} have been also observed and assigned by Bridgman [16]. The spectrum of PW_{12}/TiO_2 A sample presents the bands characteristic of the support and PW_{12}. A perusal of Fig. 2(A) indicates that for this sample no significant shift of the most sharp and intense band of PW_{12} can be observed. This band, in fact, was recorded at 1006 cm^{-1}, whereas that at 992 cm^{-1} is broadened. The peaks corresponding to P—O and W=O vibration modes are broadened with respect to the bare PW_{12} spectrum. These findings can be attributed to a H—bonding interaction between the oxygen atom of the Keggin anion and the hydroxyl groups on the TiO_2 surface, as observed before [17–19]. As far as the PW_{12}/TiO_2 ex A sample is concerned, the Raman spectrum evidences that the Keggin structure was compromised not only because the characteristic PW_{12} vibration modes are not present, but because a new band at 961 cm^{-1} appeared. The latter was attributed to a vibration mode of a strong deformed Keggin cluster structure (confirmed by FTIR investigation reported in the following). On the contrary, the structure of the Keggin cluster remained unchanged after the preparation of the binary PW_{12}/SiO_2 binary material, as reported in Fig. 2(B) because no significant shifts of the characteristic bands are observed. The slight widening of the vibration bands can be attributed to electrostatic interaction with the support. In the PW_{12}/CNT binary material (Fig. 2(C)) there is no evidence of vibrational modes of PW_{12} and only the characteristic modes of the CNT can be noticed, i.e. two main peaks: the so-called G—band (1575–1601 cm^{-1}), characteristic feature of the graphitic layers, and a second characteristic mode (D—band), typical sign for defective graphitic structures (1320–1348 cm^{-1}) [20].

FTIR experiments were also useful to evaluate the preservation of the Keggin structure in the binary materials (Fig. 3). The preservation of Keggin anions was confirmed by the bands which are due to the skeletal vibrations and were recorded in the range 1200–400 cm^{-1}. The spectrum of the bare PW_{12} showed four characteristic bands [15,16,21] at 1080, 982, 890, 810 cm^{-1} corresponding to ν_{as}(P—O_a), ν_{as}(W—O_d), ν_{as}(W—O_b—W) and ν_{as}(W—O_c—W), respectively (Fig. 3(A)). The spectra of supported PW_{12} samples were, in some cases, dominated by the SiO_2 or TiO_2 supports. The Ti-O bonds in the TiO_2 Evonik sample give rise to an absorption spectrum in the range 1300–700 cm^{-1} with a broad band in the range 900–700 cm^{-1} (Fig. 3(A)). The latter band was observed also in the binary samples containing TiO_2 (PW_{12}/TiO_2 ex A and PW_{12}/TiO_2 A). In the case of PW_{12}/TiO_2 ex A the Keggin anion vibrations were not clearly evident, the only vibration observed was ν_{as}(W-O_d), although it shifted from 982 cm^{-1} to 972 cm^{-1}. This result can be attributed to the Keggin structure deformation in agreement with the Raman spectra. On the other hand the spectra of PW_{12}/TiO_2 A was characterized by the disappearance of only the ν_{as}(W—O_c—W) vibration at 810 cm^{-1} because of the presence of the broad band of TiO_2 from 900 to 700 cm^{-1}. Therefore, for the PW_{12}/TiO_2 ex A catalyst both IR and Raman analyses evidenced a problem in the preservation of the Keggin anion structure.

In the case of silica samples (Fig. 3(B)), the bands of SiO_2 at 1105 and 1200 cm^{-1}, appeared only for the PW_{12}/SiO_2 ex A sample. The Keggin anion vibrations were observed at the same frequencies for both PW_{12}/SiO_2 ex A and PW_{12}/SiO_2 A and for the bare PW_{12}, indicating that the Keggin structure in these binary materials was preserved. As far as the CNT based materials is concerned no significant changes were observed between the bare PW_{12} and the supported samples. For PW_{12}/CNT-1 sample the ν_{as} (W—O_b—W) vibration shifted from 890 cm^{-1} to 888 cm^{-1} (Fig. 3(C)).

3.2. Catalytic and photocatalytic reactivity

3.2.1. Infra-red monitoring of 2-propanol dehydration: catalytic reactivity in system I

System I presents the in-situ monitoring of the interaction between 2-propanol and catalysts by using IR spectroscopy. The typical IR gas spectra of 2-propanol, propene and diisopropyl ether (DIPE) are reported in Fig. 4(A). During the observation of 2-propanol dehydration in *system I*, the intensities of the IR bands characteristic of this substrate decrease, while those characteristics of propene and diisopropyl ether increase. In order to follow propene evolution, two bands were chosen as diagnostic bands, i.e. those observed at 910 and 980 cm^{-1} (corresponding to ωCH_2 and ωCH bending vibrations respectively) while for DIPE evolution that at 1027 cm^{-1} (C—O stretching vibration) was monitored. These diagnostic wavenumbers have been chosen because they did not overlap with either 2-propanol or Keggin vibrations (See Fig. 4(A)). By monitoring the FTIR of the reaction evolution in *system I*, it can be observed that traces of propene (band at 980 cm^{-1}) were observed already at the lowest reaction temperature (60 °C), as it is presented in Fig. 4(B). The propene (bands at 980 and 910 cm^{-1}) began to form at 80 °C, together with DIPE (1027 cm^{-1}). For the PW_{12}/CNT-

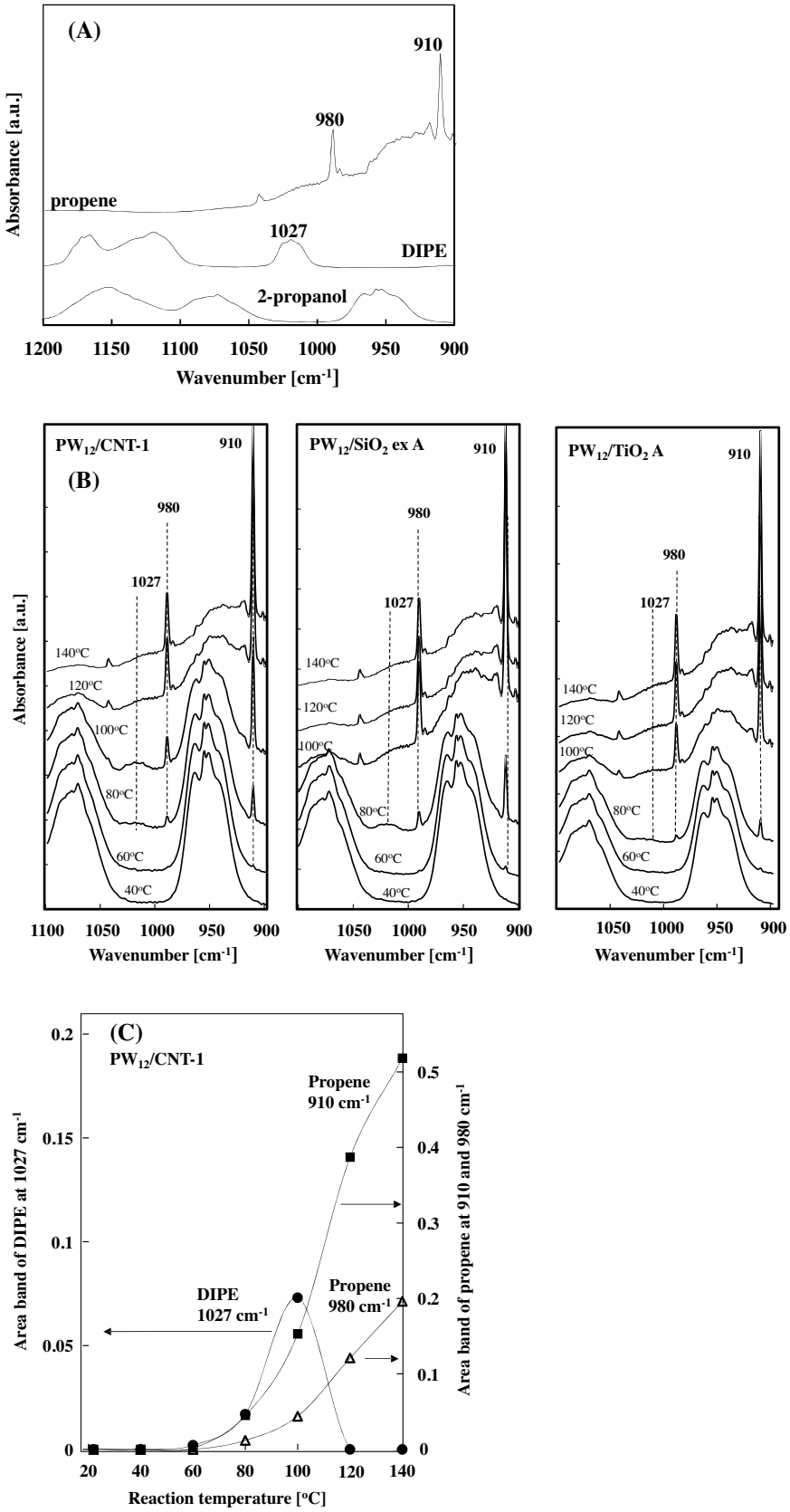

Fig. 4. (A) FTIR spectra of gas phase of 2-propanol, propene and diisopropyl ether (DIPE) in the range of 1200–900 cm^{-1}. (B) FTIR spectra of gas phase over samples: PW_{12}/CNT-1, PW_{12}/SiO_2 ex A, PW_{12}/TiO_2 A, in 2-propanol vapour at 1.3 kPa and at different reaction temperatures 40–140 °C. (Set-up *system I*). (C) The areas of DIPE (at 1027 cm^{-1}) and C3 bands (at 990 and 910 cm^{-1}) calculated from IR spectra of the gas phase over PW_{12}/CNT-1 after its interaction with 2-propanol at different reaction temperature.

1 and PW_{12}/SiO_2 ex A the amount of DIPE was increasing at first and after reaching 100 °C decreased. It is due to its decomposition either to propene or 2-propanol. This fact is clearly visible in Fig. 4(C) which presents the changes of intensities in propene (910 and 980 cm^{-1}) and DIPE bands (1027 cm^{-1}). The changes observed in the FTIR spectra can be, for convenience, quantified by monitoring the areas of the IR bands and plotting their changes versus the reaction temperature. This plot is presented, as the example, for the bands observed by using PW_{12}/CNT-1 in *system I* (Fig. 4(C)). The area of the bands attributed to propene (C3) continuously increases in the temperature range 60–140 °C, while the area of the DIPE band initially increases, reaches a maximum at 100 °C and then decreases. In fact, DIPE can decompose to form propene or 2-propanol according to Reactions (1) and (2), respectively:

$$C_3H_7OC_3H_7 \rightarrow 2C_3H_6 + H_2 \quad (1)$$

$$C_3H_7OC_3H_7 + H_2O \rightarrow 2C_3H_7OH \quad (2)$$

To confirm the possible mechanism of DIPE decomposition (by Reactions (1) or (2)), DIPE was separately adsorbed on dehydrated catalysts under the same conditions previously used for monitoring 2-propanol dehydration. No bands characteristic for 2-propanol were observed, and the maxima of C3 appeared, which confirmed the decomposition of DIPE to propene (Reaction (2)).

Since the decomposition of DIPE began at 60 °C, the temperature of 80 °C was chosen to carry out the dehydration of 2-propanol in the (photo) catalytic reactor working in a continuous gas-solid regime (*system II*).

As highlighted by Misono and co workers [13,21], heteropolyacids possess a considerable ability to dissolve water molecules and they are characterized by the presence of a significant amount of crystallization water molecules located between Keggin units. The interaction between these water molecules and the weakly bonded protons in HPA structures induces the formation of $(H_2O)_nH^+$ species (H_3O^+ and $H_5O_2^+$) which significantly influences the HPAs catalytic activity [22,23]. The FTIR spectra of supported PW_{12} before and upon 2-propanol dehydration at 80 °C in the range 1800–1600 cm^{-1} (Fig. 5) were useful to identify H_3O^+ and $H_5O_2^+$ species. The samples PW_{12}/SiO_2 ex A (spectrum a) and PW_{12}/TiO_2 A (spectrum c) before the adsorption of the alcohol were evacuated 10 min. In the spectrum of the PW_{12}/SiO_2 ex A sample, a band at 1700 cm^{-1} corresponding to $\delta(H_3O^+)$ or $\delta(H_5O_2^+)$ can be noticed, while in the case of PW_{12}/TiO_2 A only a band due to $\delta(H_2O)$ at 1615 cm^{-1} was observed. Upon the interaction with 2-propanol at 80 °C the band at 1700 cm^{-1} was visible for both samples (spectra b and d). The water which is formed by 2-propanol dehydration is bonded by HPAs protons and forms $(H_2O)_nH^+$ species. By taking into account these experiments we propose the participation of H_3O^+ and $H_5O_2^+$ species in the reaction pathway presented in Scheme 1(A) and (B).

3.2.2. *Catalytic and catalytic photo-assisted 2-propanol dehydration (Set-up* system II*)*

System II allows to compare the reactivity of the various (photo) catalysts versus 2-propanol dehydration. Preliminary runs indicated that the presence of the heteropolyacid is essential for the conversion of 2-propanol both in catalytic and photocatalytic reactions; in fact, no activity was observed in the presence of materials where PW_{12} was absent. As far as the temperature is concerned, the occurrence of the reaction needed $T \geq 60$ °C both under irradiation and dark conditions. Some preliminary runs were carried out at increasing volumetric flow rates with the same initial concentration of 2-propanol (1 mM) to establish the minimum feeding volumetric flow of gaseous mixture of 2-propanol and N_2 to avoid transport phenomena limitations. The reaction rates of propene formation measured during a run carried out in the presence of

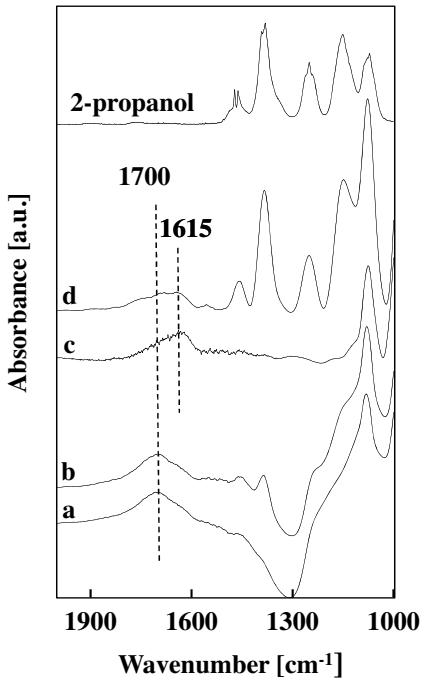

Fig. 5. FTIR spectra of PW_{12}/SiO_2 ex A (spectra a,b) and PW_{12}/TiO_2 A (spectra c,d) samples: before 2-propanol sorption (a,c), in 2-propanol vapour at 1.3 kPa and 80 °C (b,d).

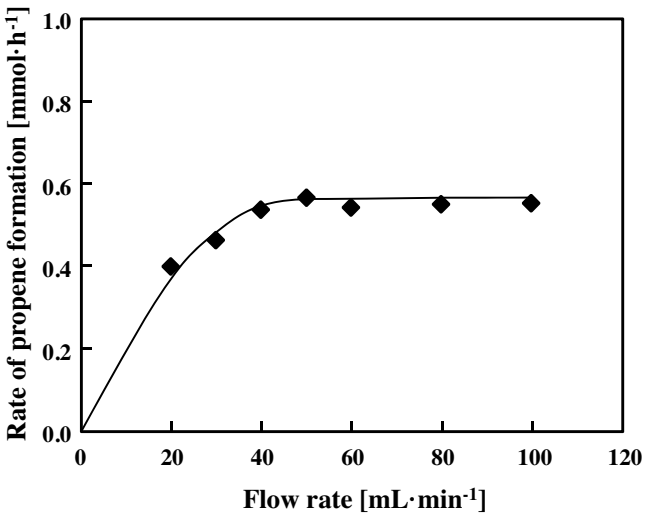

Fig. 6. Reaction rate of propene formation versus the flow rate of feeding gas for runs carried out under irradiation by using PW_{12}/TiO_2 A as the catalyst. 2-propanol concentration in the feeding gas equal to 1 mM. Runs carried out under irradiation. (Set-up called *system II*).

PW_{12}/TiO_2 A sample, are reported in Fig. 6. A plateau of the reaction rate was reached at a flow rate of ca. 50 mL·min^{-1}. Consequently the (photo) reactor was fed at 100 mL min^{-1} and this high flow value allowed to work under kinetic regime conditions for all of the catalysts used. Some additional preliminary experiments carried out at different 2-propanol concentrations and by using three selected (photo) catalysts in the dark and in the presence of light are reported in Fig. 7(A) and (B), respectively.

As the active (photo) catalytic species responsible for 2-propanol dehydration was HPA, to compare the reactivity of the various catalysts used, in the following the results are reported per gram of PW_{12} present in the binary material.

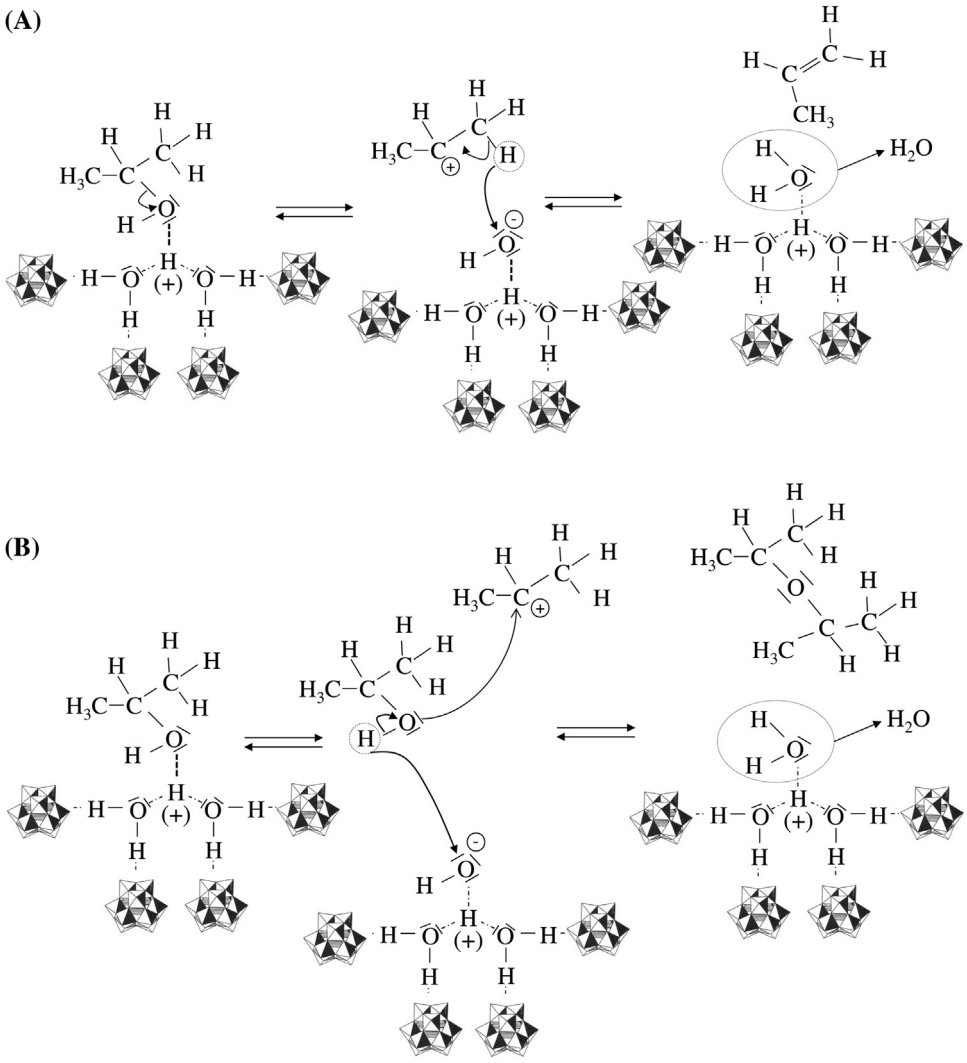

Scheme 1. Proposed reaction pathway for the catalytic 2-propanol dehydration to obtain (A) propene and (B) diisopropyl ether, in the presence of the Brönsted acidic species on the heteropolyacid catalysts.

A perusal of Fig. 7(A) and (B) indicates that by increasing the concentration of 2-propanol in the gas phase fed to the reactor, the rate of propene formation firstly increased up to reaching a maximum and then decreased to very low values getting a plateau for concentrations equal or higher than 2 mM.

The maximum value of propene rate formation depended on the catalyst used and it was higher for runs carried out under irradiation. In particular, the concentration of 2-propanol corresponding to the maximum reactivity for propene formation ranged between 0.1 and 0.5 mM, depending on the catalyst used and on the presence or absence of light during the run. This behaviour of the catalysts is unusual in catalysis; indeed, the reactivity increased by increasing the substrate concentration reaching a plateau for high amounts of substrate. In this study, however, it must be considered that the (photo) catalysts used were binary materials containing a heteropolyacid (PW_{12}) that is the active species whose presence resulted fundamental for the dehydration of 2-propanol. As reported in the literature, the bare heteropolyacid species have the ability to absorb polar substrates giving rise to catalytic reactions in a peculiar phase known as "pseudo-liquid" phase [24], described extensively by Okuhara et al. [21]. This phenomenon can be explained by invoking the solubility of polar substrates in the water molecules present between the heteropolyacid clusters (primary structures) forming the secondary structure in the solid (photo) catalysts. The absorption of the substrate in the pseudo-liquid phase is beneficial for the reactivity; however, it is reported that a substrate concentration in gas-phase exists above which the absorption onto the catalyst surface increases very much causing a dramatic decrease of reactivity [21,24,25], as observed in the present work (see Fig. 7(A) and (B)). By considering the results obtained in this study, it can be concluded that also the supported PW_{12} species, similarly to the bulk ones [21], give rise to catalytic phenomena involving the pseudo-liquid phase. The presence of UV light not only produced an increase of the catalyst activity but also a shift to higher values of 2-propanol concentration for which the reactivity reached a maximum after which it drastically decreased (see Fig. 7(A) and (B)).

As it can be observed, it is impossible to find a unique concentration of 2-propanol for which the reactivity is maximum, but the 0.5 mM concentration resulted a good compromise in order to compare the reactivity of the various samples.

Figs. 8 and 9 report the rate of propene and diisopropyl ether formation, respectively, for catalytic and catalytic photo-assisted 2-propanol dehydration reactions in the presence of bare and supported PW_{12} materials. Notably, the steady-state conditions were always achieved after few minutes and the (photo) catalytic activity was constant throughout all the tests.

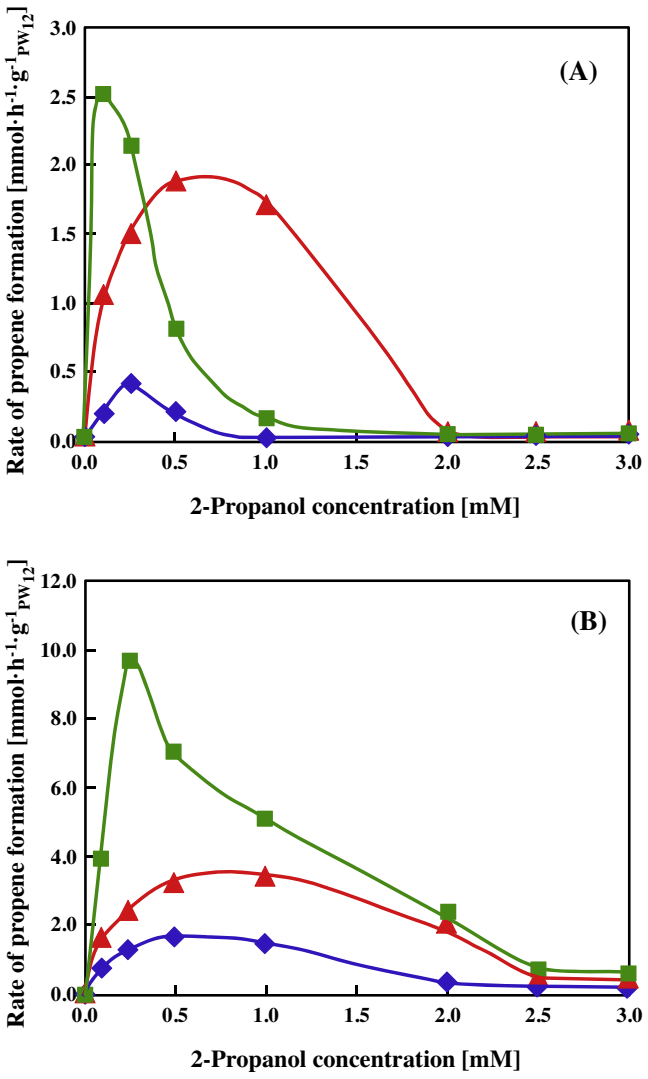

Fig. 7. Reaction rate of propene formation versus 2-propanol initial concentration for runs carried out by using (▲) PW_{12}/SiO_2 A, (■) PW_{12}/TiO_2 A and (◆) PW_{12} as the catalysts. (A) in dark condition and (B) under irradiation. Flow rate of the feeding gas equal to 100 mL min^{-1}. (Set-up called *system II*).

From a perusal of Fig. 8 it is evident that, all of the binary materials presented a better (photo) catalytic activity versus the propene formation than the bare PW_{12}, with the exception of the PW_{12}/TiO_2 ex A sample. This finding indicates that deposition of PW_{12} on SiO_2, TiO_2 and CNT was beneficial.

As far as the catalytic experiments in the absence of UV light are concerned, the catalytic reactivity of bare PW_{12} appeared to be very poor. On the contrary, when PW_{12} was present in the binary materials the reactivity per gram increased, in some cases significantly. The PW_{12}/SiO_2 A sample, in which PW_{12} was impregnated on SiO_2 under hydrothermal conditions, showed the best reactivity.

In order to explain the increase of the catalytic activity of the binary materials with respect to the bare PW_{12} it should be considered that all of the binary samples showed a higher SSA with respect to the bare PW_{12}, and consequently a larger surface of contact between the PW_{12} cluster and 2-propanol could be achieved. The interaction between PW_{12} and SiO_2, TiO_2 and CNT could enhance, as already reported for the opposite reaction (propene hydration to form 2-propanol) [26], the strength of the PW_{12} Brønsted acid sites and this fact can also account for the improvement of the reactivity of the binary system with respect to the bare PW_{12} sample. Indeed, according to the literature [27], the dehydration of 2-propanol occurs by means of an acid-base mechanism (elimination E1) involving the dioxonium ions placed between PW_{12} anions (see Scheme 1(A) and (B)). The higher reactivity observed for PW_{12}/SiO_2 A with respect to PW_{12}/SiO_2 ex A sample could be related to a better interaction with the support, due to the different preparation method and the higher amount of PW_{12} (74 versus 26%, respectively). As far as the PW_{12}/TiO_2 A and PW_{12}/TiO_2 ex A samples are concerned, the reactivity of PW_{12}/TiO_2 A was quite good and similar to that of PW_{12}/SiO_2 ex A, whereas, the PW_{12}/TiO_2 ex A sample was virtually inactive. The good activity of PW_{12}/TiO_2 A sample can be explained by the same considerations applied for PW_{12}/SiO_2 samples. On the other hand, the inactivity of the PW_{12}/TiO_2 ex A sample could be due to the preparation method that induced the PW_{12} Keggin structure degradation as evidenced by Raman (Fig. 2(A)) and FTIR (Fig. 3(A)) studies.

The strong acidity of the PW_{12} cluster which acted as catalyst for the in situ alcohol dehydration to propene during the preparation of PW_{12}/TiO_2 ex A sample, when 2-propanol deriving from hydrolysis of Ti isopropoxide formed, can account for the damage of the Keggin structure. The massive dehydration reaction, in fact, can give rise to a complete elimination of the acidity of the cluster and to its complete degradation. It is worth to mention that the pressure inside the autoclave during the preparation of PW_{12}/TiO_2 ex A increased up to 50 bar, indicating the evolution of propene gas. Pressure increased up to only 30 bar during the preparation of the PW_{12}/SiO_2 ex A sample indicating a moderate evolution of ethene that favoured the porosity of the sample (see Section 3.1).

Concerning the reactivity of the PW_{12} impregnated CNT samples, it was observed that PW_{12}/CNT-1 corresponding to a theoretical monolayer of supported PW_{12} was the most active material, although it is likely that some of the heteropolyacid was located inside the CNT network and it resulted inaccessible for 2-propanol. This hypothesis is supported by the fact that the surface areas of PW_{12}/CNT-0.5 and PW_{12}/CNT-1 samples are very similar but significantly lower than that of the bare CNT (138 $m^2\ g^{-1}$) and higher than that of the bare PW_{12} (15 $m^2\ g^{-1}$).

Therefore, it is plausible that a fraction of PW_{12} filled the nanotubes reducing the surface area of CNT. The XRD pattern, along with the Raman and FTIR spectra of PW_{12}/CNT-0.5 samples (not reported for the sake of brevity), showed very low signals attributable to the presence of PW_{12} indicating that part of the heteropolyacid could fill the nanotubes. Notably lines in XRD pattern indicate that PW_{12} (at least partially) is present as crystalline phase.

Addressing now our attention to the tests carried out in the presence of UV light, the reactivity of the samples always increased with respect to that showed under dark conditions. All considerations and trends reported for the catalytic tests can be analogously applied to the catalytic photo-assisted runs. It is important to underline that the photo-catalytic experiments were carried out using LED as source of UV light irradiation and therefore during each photo-catalytic run the temperature did not change.

Scheme 1(A) shows the hypothesized mechanism of the catalytic dehydration of 2-propanol to propene. As demonstrated by Misono and co workers, heteropolyacids possesses a discrete and mobile ionic structure that can retain in the bulk a large amount of polar water molecules with very high proton mobility [13,28]. Proton on the PW_{12} surface is coordinated by two water molecules forming the di-aqua-proton species dioxonium, $H_5O_2^+$, and these species form bridges between the Keggin ions units. Ivanov et al. proposed that the role of active centers in propene hydration reaction catalyzed by heteropolyacids is played by $H_5O_2^+$ [23]. The $H_5O_2^+$ sites contribute to stabilize the polar water molecules with formation of the "pseudo-liquid" phase. The structures of binary catalysts characterize the presence of such species which was confirmed by IR experiments (Fig. 5). Consequently, the reaction occurs between 2-propanol from the gas phase and dioxonium ions sit-

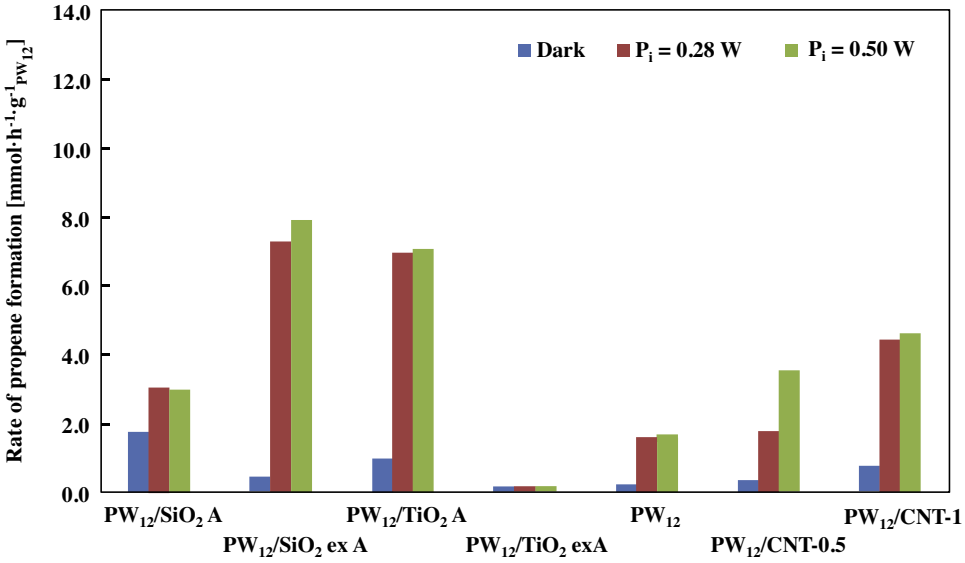

Fig. 8. Propene formation rate per gram of PW_{12} for the catalytic and catalytic photoassisted 2-propanol dehydration reaction by using the set-up called *system II*. Temperature equal to 80 °C. 2-propanol concentration in the feeding gas equal to 0.5 mM.

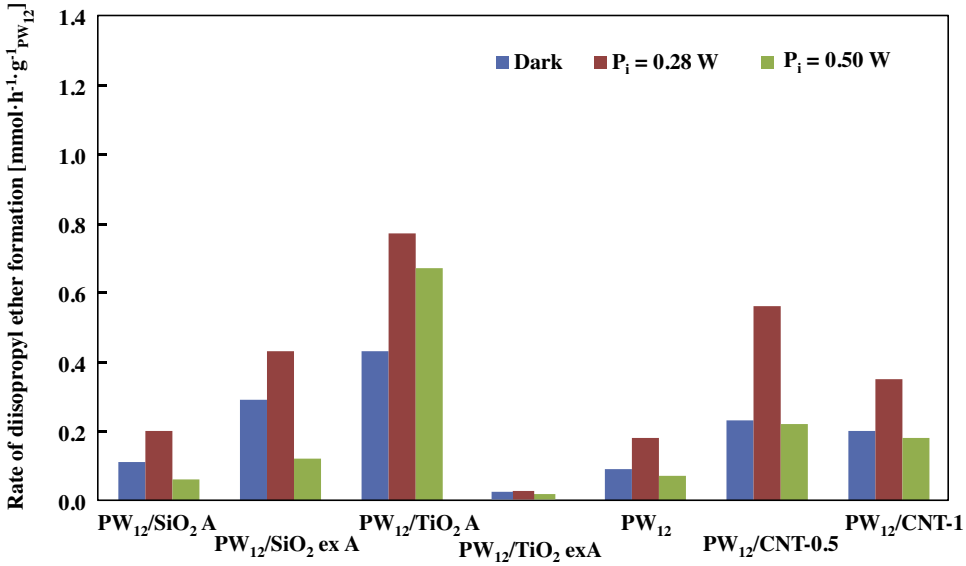

Fig. 9. Diisopropyl ether formation rate per gram of PW_{12} for the catalytic and catalytic photoassisted 2-propanol dehydration reaction by using the set-up called *system II*. Temperature equal to 80 °C. 2-propanol concentration in the feeding gas equal to 0.5 mM.

uated between Keggin anions. According to Ivanov et al. a direct correlation between the reactivity and the acidity of the surface in terms of amount of $H_5O_2^+$ is the key factor to obtain the maximum activity. Analogous reaction mechanism for the catalaytic 2-propanol dehydration in the presence of HPA has been reported by Bond et al. [27].

During the catalytic and catalytic photo-assisted experiments also the formation of diisopropyl ether occurred along with propene formation (see Scheme 1B).

In order to understand why the PW_{12} acts as a photoactive material, it is necessary to consider the electronic consequences of this cluster irradiation. The HPA species are typically fully oxidised (d° electron configuration on the addenda metal centers) and the light absorption in this system is mainly attributed to ligand to-metal charge transfer (LMCT) bands (oxygen to metal) in the wavelength region 200–500 [29,30]. An electron is promoted from a spin-paired, doubly occupied bonding orbital (HOMO) to an empty, antibonding orbital (LUMO), resulting in the generation of an oxo-centered radical [31]. The photoexcited cluster species formed (indicated as PW_{12}^*) is highly reactive and it is both a better oxidizing agent (higher electron affinity) and a better reducing agent (lower ionisation energy) than the corresponding ground-state species. Consequently, during the catalytic photo-assisted reactions, in addition to the previous mentioned acid-base mechanism, a further key role is played by PW_{12}. Indeed, PW_{12} after photosensitation to PW_{12}^* can trap an electron from 2-propanol reducing to the blue species (PW_{12}^-) [22,30]. Notably, all the materials containing PW_{12} become strongly blue coloured under irradiation only in the presence of 2-propanol. The further hypothesized evolution of 2-propanol radical species to propene is reported in Scheme 2. Notably, very small amounts of acetone were also detected in the initial stages of the reaction, probably due to the presence of traces of adsorbed O_2.

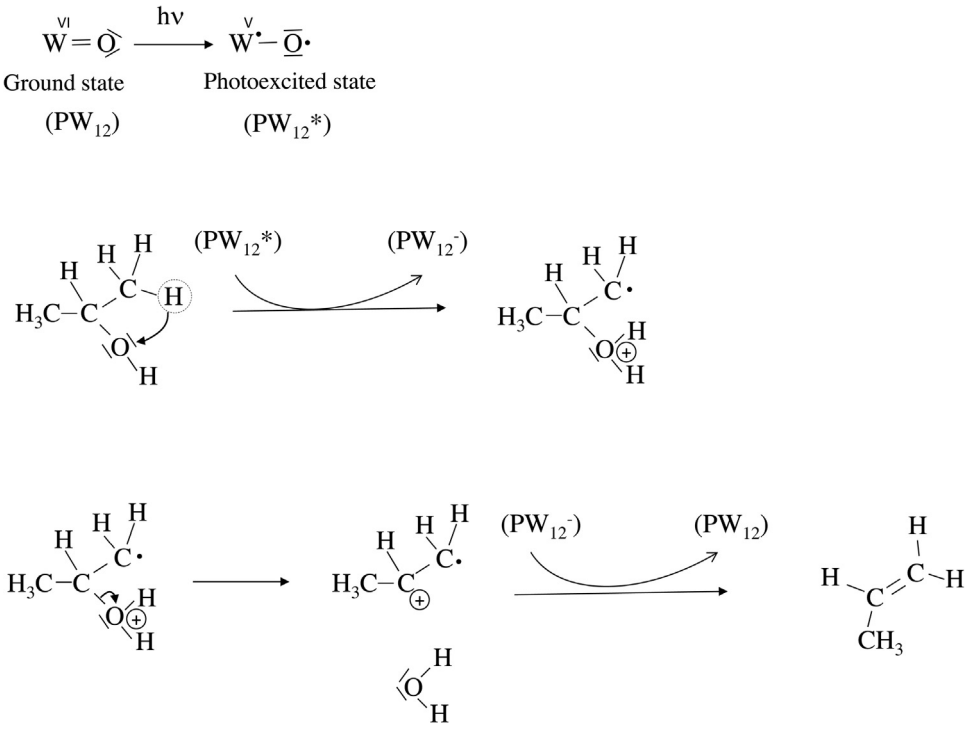

Scheme 2. Proposed reaction pathway for the catalytic photo-assisted 2-propanol dehydration to propene occurring along with the catalytic reaction (Scheme 1) in the presence of the materials containing PW_{12}.

Moreover, in order to explain the higher activity of the heteropolyacid based materials under irradiation conditions, a change of their acidity can be also invoked, due to their reduction to PW_{12}^{-} The formation of the latter species depends on the pH values of the reaction medium [30,32]. From the perusal of Fig. 8 and by comparing the PW_{12}/SiO_2 A and PW_{12}/TiO_2 A samples (samples prepared by following the same method), it is evident that the presence of light caused a higher increase of the reactivity in the case of the sample in which PW_{12} was deposited on TiO_2. In a previous paper [33], the different beneficial influence of light on the photoreactivity of various HPA supported materials for the propene hydration (the reverse reaction here studied) was reported and it was suggested the occurrence of a synergistic effect only when the heteropolyacid was coupled with a semiconductor such as TiO_2. Indeed, the photoexcited (PW_{12}^{*}) possesses an oxidation potential sufficient to abstract a photogenerated electron from the conduction band of TiO_2. Such electron transfer could (i) produce a higher number of PW_{12}^{-} species inducing an increase of the reaction rate of 2-propanol dehydration and (ii) inhibit the fast electron-hole recombination on TiO_2 (see Scheme 3).

On the other hand, the extraordinary increase of reactivity observed under irradiation in the case of the PW_{12}/SiO_2 ex A sample could be explained by considering that the preparation method used gives rise to a very intimate contact between PW_{12} and SiO_2 that could strongly enhance the strength of the Brönsted acid sites under UV light irradiation. The increase of the reactivity observed when PW_{12}/SiO_2 ex A sample was irradiated resulted much higher than that observed in the case of PW_{12}/SiO_2 A. The different and apparently contradictory behaviour of these two samples under irradiation can be explained by considering that during the preparation of the PW_{12}/SiO_2 A, an amount of PW_{12} entered the pores of the SiO_2 support clogging part of them (the SSA decreases from 517 to 32 $m^2\,g^{-1}$, see Table 1). Therefore, the PW_{12} present inside the pores of this sample cannot be reached by the light and consequently the increase of the reactivity under irradiation is less significant.

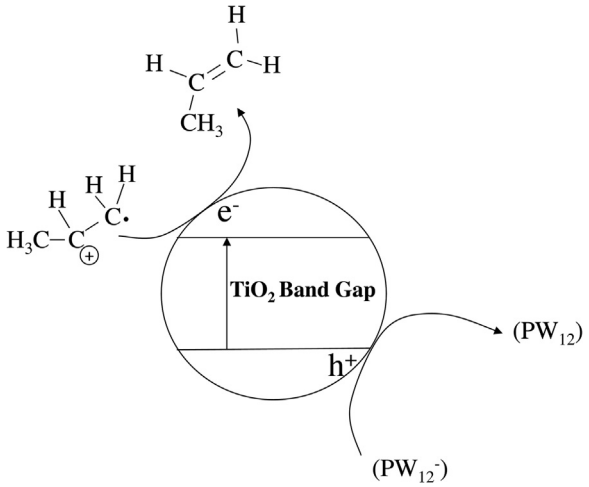

Scheme 3. Synergistic effect between the PW_{12} cluster and TiO_2 in the binary composite for the catalytic photo-assisted 2-propanol dehydration to form propene.

Results reported in Fig. 8 indicate that only a slight enhancement or no variation of the reactivity were observed by increasing (ca. doubling) the power of UV light reaching the photocatalyst. To justify these finding it can be considered that almost all the catalyst surface was virtually excited already by using the lower power irradiation source and therefore the surplus of photons had only a marginal effect.

The reaction rate of diisopropyl ether formation, both in the absence and in the presence of UV light is reported in Fig. 9. This reaction rate was generally much lower (by one order of magnitude) than that of propene formation (reported in Fig. 8). In this case the presence of UV light gave rise to an apparent contradictory effect. Indeed, an increase of the diisopropyl ether reaction rate was observed when the samples were irradiated with the lowest power light, whereas a decrease of the reactivity was observed by

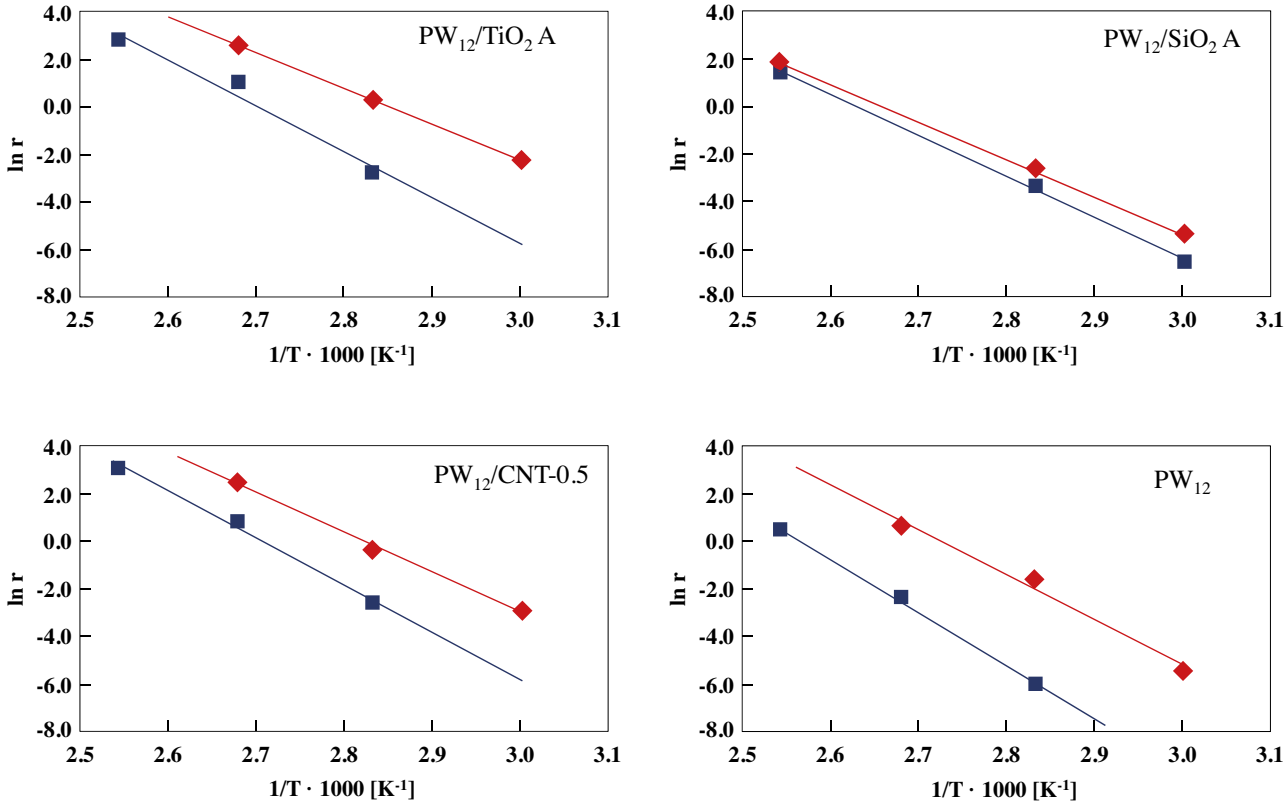

Fig. 10. Plots of "*ln r*" versus "*1/T*" used to calculate "E_a" and "*ln A*" for four selected samples. The units of "*r*" are mmol h^{-1} g^{-1} PW_{12}.

irradiating with the highest power light. It is not easy to explain this finding suggesting that when the catalysts were irradiated with the highest light power, the surplus of energy favoured the formation of propene and/or the decomposition of the formed ether.

3.2.3. *Study on the apparent activation energy in catalytic and catalytic photo-assisted 2-propanol dehydration to propene (Set-up* system II*)*

In order to estimate the apparent activation energy of 2-propanol dehydration reaction to propene, some experiments of 2-propanol dehydration were carried out at different temperatures from 60 to 120 °C by using the same 2-propanol inlet concentration (3 mM) and at the same volumetric flow rate (100 mL min^{-1}).

According to the results reported in Fig. 7(A) and (B) for concentration of 2-propanol equal or higher than 2–2.5 mM, the reaction rate was very low and constant (the conversion was less than 10%), indicating that the reaction can be considered of pseudo-zero order, under these experimental conditions. This finding was explained by considering that at high 2-propanol concentrations (>2 or >2.5 mM, depending on the catalyst) 2-propanol completely covered the catalysts surface, giving rise to a paramount absorption in the pseudo-liquid phase [21].

Therefore in this conditions the rate of propene formation can be written as:

$$r = k_0 \tag{3}$$

in which "k_0" is the pseudo-zero order rate constant of the reaction.

The apparent activation energies E_a and the pre-exponential factors *A* were determined from the Arrhenius equation in the form:

$$\ln r = \ln k_0 = \ln A - \frac{E_a}{RT} \tag{4}$$

Eq. (4) has been applied for the runs carried out both in the presence and in the absence of UV-light by using bare PW_{12} or selected binary materials in the catalytic or the photocatalytic reaction. It is worth to remind that photocatalytic reactions are usually carried out at atmospheric pressure and at room temperature because the photonic activation of the photocatalyst, which is typically a semiconductor, does not require heating. By heating the system, the adsorption process becomes the rate limiting step and consequently the activity of the system decreases. The true activation energy of the process is nil, whereas the apparent activation energy is small (few kJ/mol) in the temperature range 20–80 °C [34]. In the reactivity study reported in this work the situation is different because the heteropolyacid acts as catalyst whose activity can be enhanced by the presence of UV light and consequently the adsorption processes can be activated by the temperature. Moreover, the possibility of the formation of a pseudo-liquid phase, hindered by increasing the temperature, should be also considered.

Fig. 10 reports the plots of "*ln* k_0" vs. "*1/T*" catalytic and photocatalytic experiments carried out by using the bare PW_{12}, and three selected binary materials: PW_{12}/TiO_2 A, PW_{12}/SiO_2 A and PW_{12}/CNT-0.5. The values of E_a and ln *A* estimated by means of plots of Fig. 10 are reported in Table 2. From the perusal of Table 2 it can be concluded that the selected binary materials chosen for the comparison, showed a lower value of the apparent activation energy, E_a, with respect to the bare PW_{12} sample. This finding along with additional explanations provided in Section 3.2.2, can justify the increased reactivity observed for the binary materials. Moreover, the values of E_a calculated in the presence of UV light (photocatalytic) were always lower than those estimated in dark condition (catalytic), justifying also in this case the higher reactivity observed in the photo-assisted reactions. Notably, the change of E_a was only partially compensated by the change of the pre-exponential factor *A*. This phenomenon, known as "compensation effect", has been already observed in catalysis [35] also in the presence of HPA supported catalysts [27].

4. Conclusions

Catalytic and photocatalytic tests for 2-propanol dehydration to propene were successfully carried out by using binary materials obtained by supporting a Keggin heteropolyacid $H_3PW_{12}O_{40}$ (PW_{12}) via impregnation method and/or solvothermal treatment. (Photo) catalytic 2-propanol dehydration was studied in gas-solid regime by using a continuous (photo) reactor working at atmospheric pressure and 80 °C. Propene and diisopropyl ether were the main reaction products. The Keggin heteropolyacid species played a key role both for the catalytic and the photo-assisted catalytic reactions, indicating that the acidity of the cluster accounts for the catalytic role, whereas both the acidity of the cluster and the oxidant ability of PW_{12} were responsible for the increase of the reaction rate of the photo-assisted catalytic reaction. Moreover, the presence of a photoactive semiconductor support showed a beneficial effect to enhance the reactivity of the binary material. The increase of 2-propanol concentration in the secondary structure of PW_{12}, i.e. in the pseudo-liquid phase, gave rise to an increase of the (photo) activity up to a maximum value above which a further absorption of the reagent caused a decrease.

The apparent activation energy of 2-propanol catalytic and photocatalytic dehydration, determined in the range 60–120 °C, decreased in the presence of light for all of the (photo) catalysts used.

Acknowledgements

The authors wish to thank MIUR (Rome) and Università degli Studi di Palermo for financial support. Authors wish to thank Eng. Giorgio Conigliaro for the assistance in the XRD diffractograms recording.

Appendix A. Supplementary data

Supplementary data associated with this article can be found, in the online version, at http://dx.doi.org/10.1016/j.apcatb.2016.02.063.

References

[1] M.T. Pope, A. Müller, Angew. Chem Int. Ed. Engl. 30 (1991) 34.
[2] D. Long, E. Burkholder, L. Cronin, Chem. Soc. Rev. 36 (2007) 105.
[3] V. Kozhevnikov, Chem. Rev. 98 (1998) 171.
[4] A. Hiskia, A. Mylonas, E. Papaconstantinou, Chem. Soc. Rev. 30 (2001) 62.
[5] I.A. Weinstock, Chem. Rev. 98 (1998) 113.
[6] G. Marcì, E.I. García-López, L. Palmisano, Eur. J. Inorg. Chem. (2014) 21.
[7] G. Marcì, E. García-López, M. Bellardita, F. Parisi, C. Colbeau-Justin, S. Sorgues, L.F. Liotta, L. Palmisano, Phys. Chem. Chem. Phys. 15 (2013) 13329.
[8] T. Tachikawa, M. Fujitsuka, T. Majima, J. Phys. Chem. C 111 (2007) 5259.
[9] A. Gervasini, A. Auroux, J. Catal. 131 (1991) 190.
[10] J.E. Rekoske, M.A. Barteau, J. Catal. 165 (1997) 57.
[11] M. Ponzi, C. Duschatzly, A. Carrascull, E. Ponzi, Appl. Catal. A 169 (1998) 373.
[12] D. Haffad, A. Chambellan, J.C. Lavalley, J. Mol. Catal. A 168 (2001) 153.
[13] N. Mizuno, M. Misono, Chem. Rev. 98 (1998) 199.
[14] M.S.P. Francisco, V.R. Mastelaro, Chem. Mater. 14 (2002) 2514.
[15] C. Rocchiccioli-Deltcheff, M. Fournier, R. Franck, R. Thouvenot, Inorg. Chem. 22 (1983) 207–216.
[16] A. Bridgeman, Chem. Phys. 287 (2003) 55.
[17] Y. Guo, C. Hu, J. Mol. Catal. A: Chem. 262 (2007) 136.
[18] U. Lavrenčič Štangar, B. Orel, A. Régis, Ph. Colomban, J. Sol Gel Sci. Technol. 8 (1997) 965.
[19] C.F. Oliveira, L.M. Dezaneti, F.A.C. García, J.L. de Macedo, J.A. Dias, S.C.L. Dias, K.S.P. Alvim, Appl. Catal. A 372 (2010) 153.
[20] W. Qian, T. Liu, F. Wei, H. Yuan, Carbon 41 (2003) 1851.
[21] T. Okuhara, N. Mizuno, M. Misono, Adv. Catal. 41 (1996) 113.
[22] A. Micek-Ilnicka, A. Lubańska, D. Mucha, Catal. Lett. 127 (2009) 285.
[23] A.V. Ivanov, E. Zausa, Y. Ben Taarit, N. Essayem, Appl. Catal. A 256 (2003) 225.
[24] S. Shikata, M. Misono, Chem. Comm. (1998) 1293.
[25] A. Bielański, A. Micek-Ilnicka, Inorg. Chem. Acta 363 (2010) 4158.
[26] G. Marcì, E. García-López, L. Palmisano, D. Carriazo, C. Martín, V. Rives, Applied Catal. B 90 (2009) 497.
[27] G.C. Bond, S.J. Frodsham, P. Jubb, E.F. Kozhevnikova, I.V. Kozhevnikov, J. Catal. 293 (2012) 158.
[28] S. Shikata, M. Misono, Chem. Commun. (1998) 1293.
[29] C.L. Hill, C.M. Prosser-McCartha, in: M. Graetzel, K. Kalyanasundaram (Eds.), Photosensitization and Photocatalysis Using Inorganic and Organometallic Compounds, Kluwer Academic Publishers, Dordrecht, 1993, p. 307.
[30] E. Papaconstantinou, Chem. Soc. Rev. 18 (1989) 1.
[31] D.C. Duncan, T.L. Netzel, C.L. Hill, Inorg. Chem 34 (1995) 4640.
[32] I.V. Kozhevnikov, Catalysts for fine chemical synthesis Catalysis by Polyoxometalates, vol. 2, John Wiley and Sons, Chichester, 2002.
[33] G. Marcì, E.I. García-López, L. Palmisano, Appl. Catal. A: Gen. 421–422 (2012) 70.
[34] J.M. Herrmann, Catal. Today 53 (1999) 115.
[35] J. Escobar, J.A. De Los Reyes, T. Viveros, M. Valle-Orta, M.C. Barrera, Fuel 149 (2015) 109.